ADVANCED OPTICAL MATERIALS
www.advopticalmat.de

Edible Amorphous Structural Color

Jiao Chu, Yan Chen, Shi-Ying Tan, Yuan-Yuan Liu, Wenzhe Liu, Xiaohan Liu, Lei Shi, Haifang Wang,* Wei Li,* and Jian Zi**

Due to the scarcity of blue color in the natural food palette, synthetic blue edible colorants are commonly used in daily life. With growing awareness of environmental hazards and potential side-effect impacts of synthetic food colorants on customers' health, synthetic blue edible colorants are no longer a good choice. Here, a strategy of mixing two edible sub-microspheres, mesoporous hollow TiO_2 sub-microspheres or SiO_2 sub-microspheres and cuttlefish ink particles, is reported to produce mass amorphous photonic structures (APSs) with structural color. The hues can be tuned by controlling the size of mesoporous hollow TiO_2 sub-microspheres, and the saturation is strongly related to the proportion of cuttlefish ink particles. Cytotoxicity assays and evaluation of bioaccessibility in the simulated human digestive system further prove the safety of the blue structural colorants. The blue structural colorants exhibit high color visibility, thermostability, and reliable food safety, which are promising properties for food, drugs, and cosmetics.

1. Introduction

Color is one of the primary sensory attributes, which often plays an important role in the good appetite and attraction of food. Adding edible colorants is a common method to make the food more colorful. Safety, stability, and diversity are the crucial factors for edible colorants. Blue is particularly scarce in the color palette of food. Phycocyanin is the only blue natural food colorant composed of protein and chromophore approved by Food and Drug Administration (FDA) (Title 21 of Code of the Federal Regulations, 21 CFR §73.530). It satisfies the consumers' requirement for food safety, but is sensitive to high temperature.[1] To overcome the limitations of natural edible colorants, the synthetic edible colorant with many technological advantages, such as high stability, tinctorial strength, and low cost, is another choice.[2] As typical examples of synthetic edible colorants, FD&C Blue No.1 and FD&C Blue No.2 are approved food additives in FDA (Title 21 of Code of the Federal Regulations, 21 CFR §74.101, 102). Over the last few decades, these color additives have been used in food industry worldwide. With growing awareness of the environmental hazards and the potential side-effect impacts of synthetic food colorants on customers' health, many food and beverage companies have committed to removing synthetic colors from their products.[3] Therefore, it is necessary to explore a new strategy of preparing a series of stable, functional and safe blue edible colorants.

To introduce more kinds of blue edible colorants to the palette of food under the presumption of satisfying food safety, we seek blue structural colorants as the third blue edible colorants. Compared to pigment, structural color would not fade with the change of environmental conditions (such as light, heat, and pH) provided that the associated photonic structures are retained without changed. The use of structural color is environmentally promising since it could be composed of non-polluting material. And structural color could be adjusted by changing the relevant submicron feature size without changing the material. To exploit these advantages, substantial efforts are devoted to preparing many fantastic structural colors for a variety of applications such as anti-counterfeiting,[4–7] textiles,[8–10] colorimetric sensors,[11–15] printing,[16–22] and so on.[23–29] Due to the limitations of the inedible property of the materials used in the above studies, like polystyrene spheres and block copolymers, few researches involve in edible structural colorants have been reported until recently.[30–32]

For edible colorants, consistency with the coloring effect of the pigment and food safety are two core issues. In terms of coloring effect, structural colors based on amorphous

J. Chu, W. Liu, X. H. Liu, L. Shi, J. Zi
State Key Laboratory of Surface Physics
Key Laboratory of Micro- and Nano-Photonic Structures (Ministry of Education) and Department of Physics
Fudan University
Shanghai 200433, China
E-mail: lshi@fudan.edu.cn; jzi@fudan.edu.cn

Y. Chen, X. H. Liu, W. Li
Department of Chemistry
Laboratory of Advanced Materials
Shanghai Key Lab of Molecular Catalysis and Innovative Materials
Fudan University
Shanghai 200433, China
E-mail: welichem@fudan.edu.cn

S.-Y. Tan, Y.-Y. Liu, H. Wang
Institute of Nanochemistry and Nanobiology
Shanghai University
Shanghai 200444, China
E-mail: hwang@shu.edu.cn

L. Shi, J. Zi
Collaborative Innovation Center of Advanced Microstructures
Nanjing University
Nanjing 210093, China

The ORCID identification number(s) for the author(s) of this article can be found under https://doi.org/10.1002/adom.202102125.

DOI: 10.1002/adom.202102125

photonic structures (APSs) have the similar coloring effect with pigments. Self-assembly of different-sized spheres is a common method to obtain APSs. APSs with only short-range structures and random structures lead to vivid non-iridescent structural colors. In terms of food safety, natural ingredients or synthetic food additives for daily consumption are automatically coming to mind. Cuttlefish ink nanoparticles (CINPs), widely used in food and medical fields, is a black suspension of naturally occurring nanoparticles composed of melanin, polysaccharides, oligopeptides and so on.[33] These nanoparticles have good monodispersity, which is conducive to self-assembly. The diameter of CINPs is mainly distributed in 80–160 nm (Figure S1, Supporting Information), which is beneficial to construct APSs. The wide absorption in visible spectrum ensures the high color visibility of the structural colorants. On the other hand, in order to tune the hue, sub-microspheres of different sizes are required. Thereby synthetic food additives consisting of sub-microspheres with mature production technology are chosen. Here we take TiO_2 for an example. In fact, any other edible sub-microspheres are also applicable. Foodborne TiO_2 sub-microspheres mainly come from a TiO_2 food additive known as E171 that is commonly used in many products such as desserts, candies and gums to enhance opacity and brightness.[34,35] Considering the relatively high refractive index of TiO_2, the sizes of the solid TiO_2 sub-microspheres need to be smaller than 200 nm, which may lead to accumulation even genotoxicity in the human body. Therefore, structure of hollow sub-microsphere with a mesoporous shell is designed specially.[36] The sizes of mesoporous hollow TiO_2 sub-microspheres are between 235–325 nm, which is helpful to avoid the above food safety issues.[37–39]Moreover compared with solid sub-microspheres, this structure similar to inverse photonic glass also provides more degrees of freedom to adjust the hue of structural colors.

In this work, based on a drop-coating method, a new strategy by mixing cuttlefish ink particles (CINPs) and mesoporous hollow TiO_2 sub-microspheres is proposed to produce mass APSs with high color visibility. The hues could be tuned by controlling the inner and outside diameter of mesoporous hollow TiO_2 sub-microspheres, while the saturation is strongly related to the proportion of CINPs. SiO_2 sub-microspheres with proper size are also an ideal substitute to mesoporous hollow TiO_2 sub-microspheres (Figure S2, Supporting Information). To identify the safety of edible colorants in our experiment, cytotoxicity assays and a simulated human digestive system are designed to assess the status of blue edible colorants after entering the body. This work develops a strategy to offer safe and sophisticated blue edible colorants with tunable hue and saturation, which is expected to be applied to food, drug and cosmetics field.

2. Results and Discussion

Figure 1 shows the schematic illustration of the fabrication of APSs. Mesoporous hollow TiO_2 sub-microspheres were fabricated through an aminoethanol etching process to remove the hard template of SiO_2 sub-microspheres and produce the hollow structures, followed by calcination in air. The mesoporous shell of the TiO_2 sub-microspheres can be facilely controlled by tuning the amount of titanium butoxide (Figure S3, Supporting Information). The CINPs are taken from the fresh cuttlefish without any special treatment (Figure S4, Supporting Information). APSs is obtained by mixing mesoporous hollow TiO_2 sub-microspheres and CINPs with an appropriate concentration. Then the aqueous mixture is dropped onto a substrate, dried under room temperature (or baking temperature) and humidity. Based on

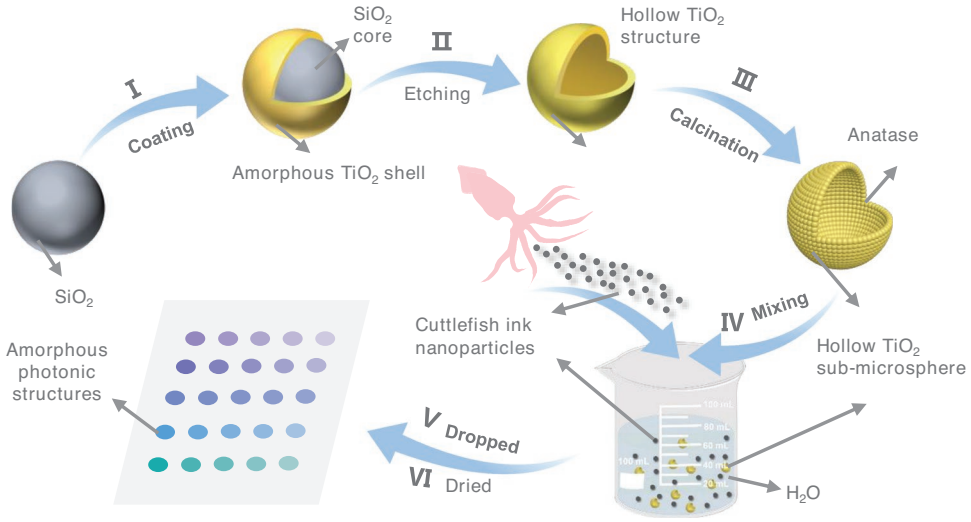

Figure 1. Schematic illustration of the fabrication of APSs. I) Synthesize the ethanol dispersible silica templates through a typical Stöber method. According to the previous report utilize some modification to prepare SiO_2@TiO_2 sub-microspheres.[36] II) Remove the hard template of SiO_2 sub-microspheres through an aminoethanol etching process to get the hollow TiO_2 structures. III) Directly annealing the as-prepared hollow TiO_2 structures at 700 °C in air for 4 h with the ramping rate of 1 °C min^{-1} to synthesize the hollow TiO_2 sub-microspheres with mesoporous shell. IV) Mix the mesoporous hollow TiO_2 sub-microspheres and CINPs with different concentrations. V,VI) Drop the mixture onto a substrate, dried under room temperature and humidity. Finally, the blue edible colorants with high visibility are obtained.

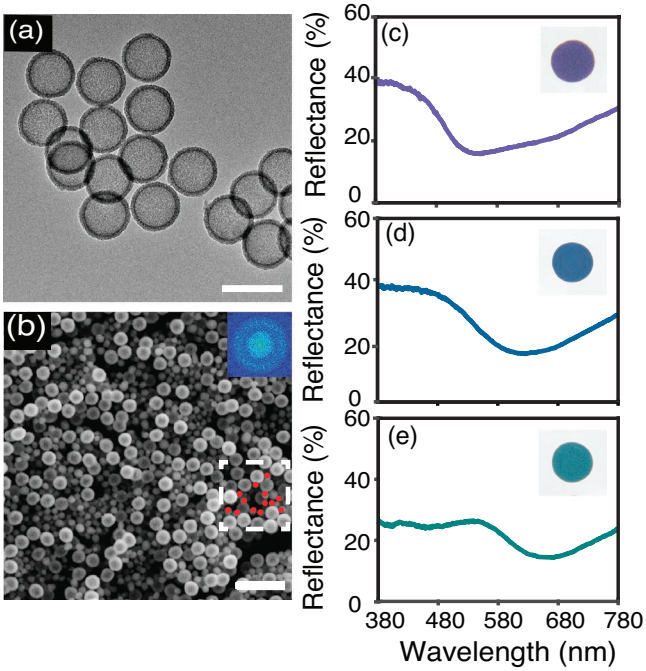

Figure 2. a) TEM image of mesoporous hollow TiO_2 sub-microspheres with inner diameter: 250 nm and shell thickness: ≈37 nm. b) SEM image of an APS composed of mesoporous hollow TiO_2 sub-microspheres with inner diameter: 170 nm and shell thickness: 33 nm mixed with CINPs. In the dashed box, ink particles are marked as red. c–e) Measured reflectance spectra for self-assembled films of APSs on a white paper with different diameters of the mesoporous hollow TiO_2 sub-microspheres (from top to bottom: inner diameter: 170, 200, and 250 nm, shell thickness: 33, 30, and 30 nm, concentration of CINPs: 0.5%, 0.5%,1.0%, the concentration of TiO_2 mesoporous hollow TiO_2 sub-microspheres is fixed on 5%.). Inset is the optical photograph of corresponding reflectance spectra. Scale bar: a) 200 nm and b) 1 µm.

the above method, a series of different hues and saturations edible structural colorants with high visibility are obtained. These structural colorants can be applied to varieties of food, drug safety-related labeling and cosmetic, highlighting the practicality and commercial value of the blue edible structural colorants.

Figure 2a shows the transmission electron microscopy (TEM) image of mesoporous hollow TiO_2 sub-microspheres. The hollow particle size and the shell thickness were determined by the TEM. Figure 2b shows the scanning electron microscope (SEM) of APS that are composed of mesoporous hollow TiO_2 sub-microspheres and modest CINPs, showing a very good structure quality with a homogeneous distribution of both particles. As shown in the inset of Figure 2b, a ring-like feature of the Fourier components reveals the structure has a well-defined short-range order. Figure 2c–e shows the reflectance spectra of three typical structural colors. With inner diameters increasing, all the spectra of the mesoporous hollow TiO_2 sub-microspheres display a broad peak, and the peak positions obviously move toward longer wavelengths. The insets of Figure 2c–e are the corresponding optical photographs, which display bluish violet, brilliant blue, and cyan blue. Obviously, the color visibility of the APSs structures is quite high. CINPs with a wide absorption in visible spectrum make a crucial contribution to the high color visibility.

Figure 3a shows color palette of blue non-iridescent structural colors with finely tunable characteristic by controlling the shell thickness, the inner diameter of the mesoporous hollow TiO_2 sub-microspheres, and the proportion of CINPs. The corresponding measured angle-resolved specular reflectance is shown in Figure S5 in the Supporting Information. The specific technical strategy is as follows. A significant change of hue could be taken by tuning the inner diameter of mesoporous hollow TiO_2 sub-microspheres. A more refined change, around a certain hue, could be taken by adjusting to the shell thickness of the mesoporous hollow TiO_2 with fixed inner diameter. The saturation of the structural color is tuned by controlling the content of CINPs. Finally, the color palette which displays from bluish violet, denim to cyan blue at different saturations is obtained. As shown in Figure 3b, to further visualize the color gamut distribution, a part of measured reflectance spectra of APSs are converted into the Commission Internationale de l'Eclairage 1931 (CIE 1931) chromaticity values. The colors of our samples are widely scattered in the blue gamut of 1931CIE. Compared with the traditional edible colorants including BBF, FD&C Blue No.2 and phycocyanin, the blue edible structural colorants expand the color gamut obviously. Regarding edible colorants industry trends, GNT, the global market leader, has announced that "Shades of Aqua" will be the key food color trend for 2020, with vivid blues and greens set to drive innovation as shoppers seek products that reconnect them with nature.[40] From the CIE, our color palette effectively expands these colors of "Shades of Aqua" (Figure S6, Supporting Information).

The mechanisms of structural colorants rely on the interaction of natural light with photonic structures whose feature sizes are comparable to the visible wavelengths. Photonic structures associated with structural color can be classified into three categories: photonic structures with long-range order and short-range order, amorphous photonic structures (APSs) with only short-range structures and random structures.[41–43] These structures, having different optical responses, result in distinctive color properties. Photonic structures display iridescent color because the bandgap is anisotropic. The pseudogap due to the short-range order is isotropic, so APSs display non-iridescent color. Random structures lack either long-range order or short-range order, causing only white color.[44]

The physical mechanism of the non-iridescent colors especially blue relies on coherent scattering of light by the amorphous structure. For most all wavelengths in amorphous structure, the path-length addition is a fraction or a non-integer number of the wavelength. These waves will be out-of-phase after scattering, so they will destructively interface with another one and cancel out. The rest of wavelengths own integer number of path-length additions after scattering in the amorphous structure. They will be in-phase waves and constructively reinforce one another to produce a wavelength-specific constructive reflection.[45] The phase relationships of scattered waves are determined by the size and spatial distribution of microparticles.[46] Short-range order makes it possible to produce consistent path-length differences between scattered waves, reinforcing limited series of wavelengths. In addition,

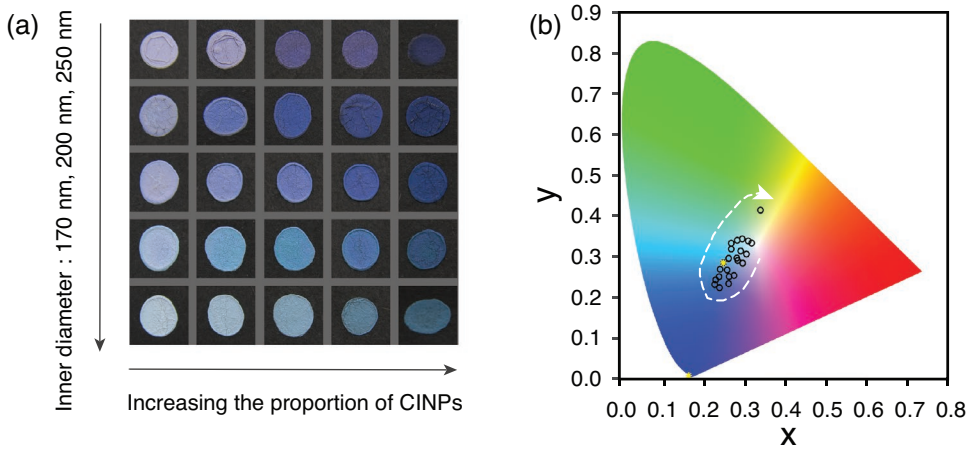

Figure 3. a) Color palette offered by the fabricated APSs. The inner diameters of mesoporous hollow TiO_2 sub-microspheres in the APSs from top to bottom are 170 nm (the first row), 200 nm (the second to the fourth row) and 250 nm (the fifth row). And the shell thickness from top to bottom is 33, 24, 27, 30, and 15 nm. In general, the thickness of the mesoporous hollow TiO_2 sub-microspheres increases from top to bottom within the same inner diameter. The proportion of the CINPs also increases from left to right: 0.0625%, 0.125%, 0.25%, 0.5%, and 1%. Each image represents a 1.5 × 1.5 cm area of the sample. b) CIE 1931 chromaticity of *x* and *y* values corresponding to the APSs. The asterisks represent the conventional blue colorants: FD&C Blue No.1 and FD&C Blue No.2.

the spatial distributions are nearly uniform in all directions because of the short-range order, so the non-iridescent colors are predicted. (Figure S7, Supporting Information).

Generally, highly ordered face-centered cubic structures will be formed by assembling of monodisperse spheres, owing to the electrostatic repulsive force. This long-range ordered arrangement will be broken down if spheres of different sizes are added in this system, eventually leading to APSs with short-range order.[47] Coherent scattering owing to the short-range order leads to photonic pseudogap, which exactly corresponds to the reflection peak. The reflection peak determines the hue. So, the hue could be tuned by controlling the size of the spheres whose feature sizes are similar to the visible spectrum (simulated analysis shown in Figure S8 in the Supporting Information). To enhance the color visibility, adding materials with wide absorption in visible wavelength is an effective method. The absorption in pseudogap is much lower than other wavelength because of lacking density of states, resulting in an overall low reflectance of the APSs. (Figure S9, Supporting Information) Finally, the APSs display vivid non-iridescent structural colors.

Edible colorants are often employed in varieties of desserts and candies for a strong visual attraction, stimulating people's desire for appetite and consumption. As shown in **Figure 4**, blue edible structural colorants are used on biscuits and donut patterns, highlighting the function of colorful decoration. In addition, the edible structural colorants also are employed in the process of baking biscuits under the temperature of 130–150 °C (Figure S10, Supporting Information). Aqueous solution of two particles is dropped on the surface of the biscuits before baking, and then dried with the baking temperature rising. In particular, the blue edible structural colorants show excellent stability to heat treatment even at 250 °C (Figure S11, Supporting Information), which is different from the color degradation of phycocyanin at high temperature. The excellent thermal stability of blue edible structural colorants is beneficial to meet the relatively wide requirements of temperature in the production of food, medicine, or other related industries. This characteristic broadens the scope of its application under high temperature conditions. While the biscuits without preservative are stored for a week under ambient temperature and humidity, the color on the surface of biscuits still keeps vivid due to the

Figure 4. Optical photographs of biscuits and donut with edible structural colorants. Scale bars: a) 2 cm, b) 1 cm.

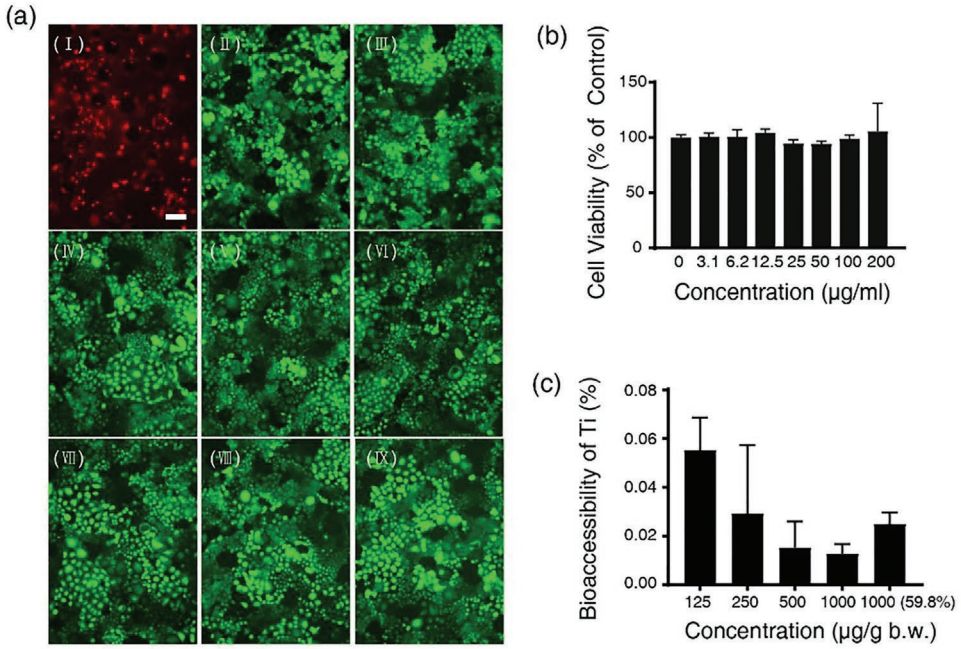

Figure 5. a) Representative live/dead staining images of Caco-2 cells after exposure to gradient concentration of edible colorant for 24 h. I) Positive control. Concentration of II–IX) 0 μg mL^{-1} (control for edible colorant), 3.1, 6.2, 12.5, 25, 50, 100, 200 μg mL^{-1}. b) Viability assay of Caco-2 cells after 24 h exposure to edible colorant with the same concentrations as a). c) The simulated absorption of TiO_2-CINPs in gastrointestinal tract in vitro by using the RIVM method. The proportion of Ti in TiO_2-CINPs is 59.60% among all samples in our experiment, except that the proportion of Ti in TiO_2-CINPs is 59.8% in the highest exposure dose in (c). Scale bar in (a): 100 μm.

natural advantages of structural color and the good stability of material (Figure S10, Supporting Information).

Although TiO_2 has been approved by FDA as an additive allowed to be added in food, and it has been reported that TiO_2 larger than 100 nm is biologically inert in both humans and animals,[34,48] we still carried out toxicity experiments on the cell level to verify that the amorphous photonic crystals in the experiment are safe. To identify the safety of edible colorants, cytotoxicity assays (**Figure 5**a,b) and evaluation of bioaccessibility in the simulated human digestive system (Figure 5c) were implemented to conduct qualitative and quantitative assessments.[49–52] Figure 5a shows the representative results, in which green spots represent live cells and red spots represent dead cells. The positive control induces a high degree of toxicity in vitro test, indicating that the toxicity observed in directed contact assay is due to the toxic components of edible structural colorants. There are almost no dead cells with the concentration of edible structural colorants increasing even at the concentration of 200 μg mL^{-1}, and the cell density does not change, indicating that edible structural colorants does not induce any toxicity. The cellular viability of Caco-2 cells after exposure to the gradient concentration of edible structural colorants for 24 h is shown in Figure 5b. All the cell viabilities are over 90%, meaning that the edible structural colorants in our experiment do not cause overt cytotoxicity, which is consistent with a). According to the previous study, the estimation of human exposure to TiO_2 is 1 mg Ti per kilogram bodyweight per day for U.S. adults and two to four times for U.S. children. Assuming an average adult weight of 75 kg or child weight of 40 kg, 75 mg Ti for an adult or 160 mg Ti for a child will be consumed each day.[34] Supposing that the area of the small intestine is 200 m^2, the density of Ti on the small intestine is 0.0375 μg cm^{-2} for an adult or 0.08 μg cm^{-2} for a child. In our assays, intestinal cells do not perform overt cytotoxicity even under the highest density of 125 μg cm^{-2} (It is corresponding to the concentration of 200 μg mL^{-1}), which is 1563-fold higher than the actual estimation for a child exposure to TiO_2. Figure 5c shows the simulated absorption of TiO_2-CINPs in gastrointestinal tract in vitro by RIVM method. The highest bioaccessibility is less than 0.06%, and the absorption usually is less than the bioaccessibility, indicating that the sample in our experiment is safe.[53] Our assays demonstrate that the edible structural colorants could be a potential edible additive, but more assessments are still needed for actual application.

3. Conclusion

In conclusion, an edible structural colorant between blue and green is proposed and demonstrated by mixing CINPs and hollow TiO_2 sub-microspheres or SiO_2 sub-microspheres to produce APSs. The edible structural colorants are with flexible adjustment. We can obtain different hues by controlling the diameter of hollow TiO_2 sub-microspheres or SiO_2 sub-microspheres and different saturations by controlling the proportion of CINPs. These edible colorants display an excellent visibility and thermal stability. A series of biotoxicity assay confirm that the edible structural colorant does not cause overt cytotoxicity, indicating that it could be a potential blue even green edible colorant for food, drug and cosmetics fields.

4. Experimental Section

Synthesis of Mesoporous Hollow TiO_2 Sub-Microspheres: Synthesis of SiO_2 Sub-Microspheres: The ethanol dispersible silica templates were synthesized through a typical Stöber method. Briefly, ethanol (74 mL), water (10 mL), and ammonium hydroxide (3.0 mL) were mixed with magnetic stirring (550 rpm, 15 min). Afterward, 1.0 mL of tetraethyl orthosilicate (TEOS) were added, and the mixed solution was continually magnetic stirred for 15 min at room temperature (22 °C). Subsequently, 3.0 mL of TEOS were added to the reaction system and allowed to proceed for 4 h. Then, SiO_2 sub-microspheres were separated by centrifugation at 8000 rpm for 5 min, washed three times with deionized water, and ethanol, and then dispersed in 20 mL of ethanol (50 mg mL^{-1}).

Synthesis of $SiO_2@TiO_2$ Sub-Microspheres: $SiO_2@TiO_2$ sub-microspheres were prepared according to the previous report with some modification. In a typical synthesis, an ethanol dispersion of the SiO_2 sub-microspheres (1.0 mL, 50 mg mL^{-1}) were dispersed in absolute ethanol (70 mL), deionized water (10 mL) and sonicated for 30 min. Then, ammonium hydroxide (1 mL) was added and magnetic stirred at 700 rpm for 30 min. Afterward, titanium butoxide TBOT (1.0 mL) were added dropwise in 5 min, and the reaction was maintained for 24 h at room temperature under stirring. The obtained $SiO_2@TiO_2$ sub-microspheres were collected by centrifugation, washed with ethanol, and dispersed in 20 mL of ethanol.

Synthesis of Mesoporous Hollow TiO_2 Sub-Microspheres: Typically, an ethanol dispersion of the $SiO_2@TiO_2$ sub-microspheres was centrifuged, washed with deionized water, dispersed in a solution containing deionized water (70 mL) and aminoethanol (70 mL) and sonicated for 15 min. Subsequently, the mixture was subjected to treatment at 100 °C for 24 h. Afterward, the as-prepared hollow TiO_2 structures were collected and washed by deionized water and absolute ethanol for three times, respectively. The obtained products were dried at 60 °C for 6 h in an oven. Finally, mesoporous hollow TiO_2 sub-microspheres were synthesized by directly annealing the as-prepared hollow TiO_2 structures at 700 °C in air for 4 h with the ramping rate of 1°C min^{-1}.

Fabrication of APSs: Materials and Methods: Mesoporous hollow TiO_2 sub-microspheres were obtained as above methods. (inner diameter: 170 nm, outside diameter: 33 nm; inner diameter: 200 nm, outside diameter: 26, 24, and 30 nm; inner diameter: 250 nm, shell thickness: 15, 30, and 38 nm). The CINPs was taken from cuttlefish bought from market. Monodisperse SiO_2 spheres suspensions (CV ≤ 5%, 10% solids by weight) were purchased from EPRUI Biotech Co., Ltd.

The APSs were fabricated as following process: Firstly, 10 mg of dried powder CINPs were dispersed into 1 g of deionized water, and then ultrasonicated for 30 min. Gradient dilution method was used to obtain CINPs solution of 1%, 0.5%, 0.25%, 0.125%, 0.0625%, 0.0313%, 0.0160%. Secondly, 250 mg powder of mesoporous hollow TiO_2 sub-microspheres with different sizes was dispersed into 5 g deionized water and ultrasonicated for 30 min, respectively. Thirdly, 30 µL CINPs suspension of different concentrations was dropped into 30 µL mesoporous hollow TiO_2 sub-microspheres solution with different sizes, respectively. The mixed suspensions were ultrasonicated for 10 min. Finally, a small amount of the mixed suspensions was dropped onto black round photopapers and structural colorants would be obtained through natural-evaporation.

Similarly, 10 µL CINPs solution of 0.4% was dropped into the purchased monodisperse SiO_2 spheres suspensions (50 µL for 250 nm and 100 µL for 300 nm). Then, the mixed suspensions were onto white round photopapers and left 8 h for drying. Finally, structural colorants of green and blue were obtained.

Optical and Structural Characterization: The optical photographs were taken by digital camera (Canon EOS 5D). The white balance was corrected by standard 18% gray card. The microstructures of APSs were characterized by scanning electron microscope (SEM) (Sigma 300).

Spectra Measurement: The angle-resolved reflectance and scattering spectra of different structural colorant samples were measured with the R1 angle-resolved spectroscopy system (Idea Optics Co). A standard white board (250–1500 nm, reflectance > 98%) for structural colorant samples was used as reference.

Cytotoxicity Assays: Cell Line and Cell Culture: The human colon colorectal adenocarcinoma cell line Caco-2 (ATCC, NO. TCHU146) was obtained from the National Collection of Authenticated Cell Cultures (Shanghai, China).

Caco-2 cells were cultured in high glucose DMEM (4.5 g L^{-1} glucose) supplemented with 20% fetal bovine serum (FBS, Sigma-Aldrich, USA) and 1% penicillin/streptomycin. Cells were cultured at 37 °C in a humidified atmosphere of 5% CO_2/95% air.

Viability of Caco-2 Cells after Exposure to TiO_2-CINPs: Caco-2 cells (10 000 per well) in 100 µL culture medium were plated in 96-well plates (Promethe, China) and incubated for 24 h at 37 °C under an atmosphere with 5% CO_2. Then the culture medium was removed, and 200 µL of fresh culture medium containing 0, 3.1, 6.2, 12.5, 25, 50, 100, or 200 µg mL^{-1} of Ti (exist in TiO_2-CINPs) was added into the wells. After 24 h, the culture medium was eliminated and the cells were used for the viability assay.

The WST-8 cell counting kit (CCK-8, Dojindo, Japan) was used to measure the viability of cells. The cells above were washed with D-Hanks balanced salt solution and then CCK-8 solution (100 µL, containing 10% CCK-8) was added and incubated for 40 min at 37 °C. Then, the optical density (OD) of each well at 450 nm was recorded on a microplate reader (Thermo, Varioskan Flash, USA). The cell viability (% of control) is expressed as the percentage of $(OD_{test} - OD_{blank})/(OD_{control} - OD_{blank})$, where OD_{test} is OD of cells exposed to TiO_2-CINPs, $OD_{control}$ is OD of the control and OD_{blank} is OD of the well without cells. Six replicates were used and the results are presented as mean values ± standard deviation.

Live/Dead Staining of Caco-2 Cells after Exposure to TiO_2-CINPs: The cells exposed to TiO_2-CINPs were also imaged directly after staining using a live/dead viability kit (L-3224, Invitrogen, USA). The dyes in the kit, namely calcein AM and propidium iodide (PI), can differentiate live (green, Ex 495 nm/Ex 515 nm) cells from dead (red, Ex 528 nm/Ex 617 nm) cells. Cells were plated and treated with TiO_2-CINPs as described in the cell viability assay. After 24 h incubation, the culture medium was removed. The dyes dissolved in D-Hanks were introduced to cells and incubated for 30 min at room temperature, and then investigated under a fluorescence microscope (DMI3000, Leica, Germany). As the positive control, a subset of wells was treated with 3% H_2O_2 (Sinopharm, Shanghai, China) for 10 min before the dyes staining.

In Vitro Evaluation of Bioaccessibility: The bioaccessibility of titanium was investigated using the in vitro digestion model suggested in the Rijksinstituut Voor Volksgezondheid Enmilieu (RIVM) method. The RIVM model used in this study included gastric phase and intestinal phase. The composition of gastric simulation fluid, bile simulation fluid, and intestinal simulation fluid in the RIVM method is shown in Table S1 in the Supporting information. The pH of these artificial fluids was adjusted with 1 M HCl and $NaHCO_3$. All chemicals and reagents were of ultrapure quality and obtained from Sigma-Aldrich and Merck to minimize the contribution of trace heavy metals from these chemicals.

To simulate the real food intake situation, different amounts of TiO_2-CINPs were mixed with the ground and sieved (14 mesh) mouse food (Shilin Biotechnology Co., Ltd, China) to prepare samples of 781.25 µg g^{-1} food (125 µg (g b.w.)$^{-1}$), 1562.5 µg g^{-1} food (250 µg (g b.w.)$^{-1}$), 3125 µg g^{-1} food (500 µg (g b.w.)$^{-1}$), and 6250 µg g^{-1} food (1000 µg (g b.w.)$^{-1}$) TiO_2-CINPs-mouse food mixture (calculated based on the daily consumption of 4 g food per mouse). Then 0.1 g of the samples was mixed with 4 mL of the prepared gastric solution in a 15 mL polypropylene tube. The tube was shaken on a shaker (100 rpm, SPH-100B, Shanghai, China) at 37 °C for 2 h. Then, 4 mL of the intestinal solution and 2 mL of the bile solution were added to the mixture and the pH of the sample was adjusted to 6.5. Later, the sample was shaken for another 2 h and then centrifuged (3500 rpm, 10 min). After that, the Ti content in the supernatant was measured by ICP-MS (Elan DRC-e, PerkinElmer, USA). The Ti bioaccessibility is calculated following the formula below.

Three replicates were used and the results are presented as mean values ± standard deviation.

$$\text{Bioaccessibility} = \frac{\text{Total Ti in the supernatant}}{\text{Total Ti in the simulation system}} \times 100\% \quad (1)$$

Supporting Information

Supporting Information is available from the Wiley Online Library or from the author.

Acknowledgements

J.C. and Y.C. contributed equally to this work. The work was supported by the National Key R&D Program of China (2018YFE0201701, 2016YFA0201600, and 2018YFA0306201) and the National Science Foundation of China (11774063, 11727811, 91750102, and 91963212). L.S. was further supported by the Science and Technology Commission of Shanghai Municipality (19XD1434600, 2019SHZDZX01, 19DZ2253000, and 20501110500).

Conflict of Interest

The authors declare no conflict of interest.

Data Availability Statement

The data that supports the findings of this study are available in the supplementary material of this article.

Keywords

amorphous photonic structures, blue edible colorants, food safety, structural colors

Received: October 3, 2021
Revised: November 5, 2021
Published online:

[1] G. Martelli, C. Folli, L. Visai, M. Daglia, D. Ferrari, *Proc. Biochem.* **2014**, *49*, 154.
[2] W. Lian, M. Fan, T. Li, X. Zhang, Z. Rao, Y. Li, H. Qian, H. Zhang, X. Qi, L. Wang, *Ind. Crops Prod.* **2019**, *142*, 111862.
[3] R. Cortez, D. A. Luna-Vital, D. Margulis, E. Gonzalez de Mejia, *Compr. Rev. Food Sci. Food Saf.* **2017**, *16*, 180.
[4] P. Dai, Y. Wang, X. Zhu, H. Shi, Y. Chen, S. Zhang, W. Yang, Z. Chen, S. Xiao, H. Duan, *Nanotechnology* **2018**, *29*, 395202.
[5] T. H. Zhao, R. M. Parker, C. A. Williams, K. T. Lim, B. Frka-Petesic, S. Vignolini, *Adv. Funct. Mater.* **2019**, *29*, 1804531.
[6] X. Yao, Y. Bai, Y. J. Lee, Z. Qi, X. Liu, Y. Yin, *J. Mater. Chem. C* **2019**, *7*, 14080.
[7] Z. Li, Y. Liu, M. Marin, Y. Yin, *Nano Res.* **2020**, *13*, 1882.
[8] Y. Y. Diao, X. Y. Liu, *Adv. Mater. Res.* **2012**, *441*, 183.
[9] Q. Li, Y. Zhang, L. Shi, H. Qiu, S. Zhang, N. Qi, J. Hu, W. Yuan, X. Zhang, K.-Q. Zhang, *ACS Nano* **2018**, *12*, 3095.
[10] J. Chu, J. Wang, J. Wang, X. Liu, Y. Zhang, L. Shi, J. Zi, *Chin. Opt. Lett.* **2021**, *19*, 051601.
[11] Y. Takeoka, M. Iwata, T. Seki, K. Nueangnoraj, H. Nishihara, S. Yoshioka, *Langmuir* **2018**, *34*, 4282.
[12] G. Kamita, B. Frka-Petesic, A. Allard, M. Dargaud, K. King, A. G. Dumanli, S. Vignolini, *Adv. Opt. Mater.* **2016**, *4*, 1950.
[13] Y. Zhang, P. Han, H. Zhou, N. Wu, Y. Wei, X. Yao, J. Zhou, Y. Song, *Adv. Funct. Mater.* **2018**, *28*, 1802585.
[14] H. Wang, K.-Q. Zhang, *Sensors* **2013**, *13*, 4192.
[15] Q. Li, Q. Zeng, L. Shi, X. Zhang, K.-Q. Zhang, *J. Mater. Chem. C* **2016**, *4*, 1752.
[16] L. Cui, Y. Li, J. Wang, E. Tian, X. Zhang, Y. Zhang, Y. Song, L. Jiang, *J. Mater. Chem.* **2009**, *19*, 5499.
[17] Y. Wang, M. Zheng, Q. Ruan, Y. Zhou, Y. Chen, P. Dai, Z. Yang, Z. Lin, Y. Long, Y. Li, N. Liu, C.-W. Qiu, J. K. W. Yang, H. Duan, *Research* **2018**, *2018*, 8109054.
[18] A. B. Christiansen, E. Højlund-Nielsen, J. Clausen, G. P. Caringal, N. A. Mortensen, A. Kristensen, in *Nanostructured Thin Films VI*, International Society For Optics and Photonics, Bellingham, Washington **2013**, p. 881803.
[19] S. Daqiqeh Rezaei, Z. Dong, J. You En Chan, J. Trisno, R. J. H. Ng, Q. Ruan, C.-W. Qiu, N. A. Mortensen, J. K. Yang, *ACS Photonics* **2020**, *8*, 18.
[20] E. Højlund-Nielsen, J. Weirich, J. Nørregaard, J. Garnaes, N. A. Mortensen, A. Kristensen, *J. Nanophotonics* **2014**, *8*, 083988.
[21] M. Kohri, *Polym. J.* **2019**, *51*, 1127.
[22] W. Luo, Q. Cui, K. Fang, K. Chen, H. Ma, J. Guan, *Nano Lett.* **2018**, *20*, 803.
[23] L. Kong, Y. Feng, W. Luo, F. Mou, K. Ying, Y. Pu, M. You, K. Fang, H. Ma, J. Guan, *Adv. Funct. Mater.* **2020**, *30*, 2005243.
[24] J. D. Forster, H. Noh, S. F. Liew, V. Saranathan, C. F. Schreck, L. Yang, J.-G. Park, R. O. Prum, S. G. Mochrie, C. S. O'Hern, H. Cao, E. R. Dufresne, *Adv. Mater.* **2010**, *22*, 2939.
[25] P. V. Braun, *Nature* **2011**, *472*, 423.
[26] R. Ohnuki, M. Sakai, Y. Takeoka, S. Yoshioka, *Langmuir* **2020**, *36*, 5579.
[27] W. Zhang, H. Wang, H. Wang, J. Y. E. Chan, H. Liu, B. Zhang, Y.-F. Zhang, K. Agarwal, X. Yang, A. S. Ranganath, H. Y. Low, Q. Ge, J. K. W. Yang, *Nat. Commun.* **2021**, *12*, 112.
[28] C. Zhang, J. Jing, Y. Wu, Y. Fan, W. Yang, S. Wang, Q. Song, S. Xiao, *ACS Nano* **2019**, *14*, 1418.
[29] S. Sun, W. Yang, C. Zhang, J. Jing, Y. Gao, X. Yu, Q. Song, S. Xiao, *ACS Nano* **2018**, *12*, 2151.
[30] D.-P. Song, T. H. Zhao, G. Guidetti, S. Vignolini, R. M. Parker, *ACS Nano* **2019**, *13*, 1764.
[31] Z.-Z. Gu, H. Uetsuka, K. Takahashi, R. Nakajima, H. Onishi, A. Fujishima, O. Sato, *Angew. Chem.* **2003**, *115*, 922.
[32] C. H. Barty-King, C. L. C. Chan, R. M. Parker, M. M. Bay, R. Vadrucci, M. De Volder, S. Vignolini, *Adv. Mater.* **2021**, *33*, 2102112.
[33] R.-H. Deng, M.-Z. Zou, D. Zheng, S.-Y. Peng, W. Liu, X.-F. Bai, H.-S. Chen, Y. Sun, P.-H. Zhou, X.-Z. Zhang, *ACS Nano* **2019**, *13*, 8618.
[34] X. Cao, Y. Han, M. Gu, H. Du, M. Song, X. Zhu, G. Ma, C. Pan, W. Wang, E. Zhao, T. Goulette, B. Yuan, G. Zhang, H. Xiao, *Small* **2020**, *16*, 2001858.
[35] E. Baranowska-Wójcik, D. Szwajgier, P. Oleszczuk, A. Winiarska-Mieczan, *Biol. Trace Elem. Res.* **2020**, *193*, 118.
[36] W. Li, J. Yang, Z. Wu, J. Wang, B. Li, S. Feng, Y. Deng, F. Zhang, D. Zhao, *J. Am. Chem. Soc.* **2012**, *134*, 11864.
[37] B. K. Bernard, M. R. Osheroff, A. Hofmann, J. H. Mennear, *J. Toxicol. Environ. Health, Part A* **1990**, *29*, 417.
[38] J. L. Chen, W. E. Fayerweather, *J. Occup. Med. Off. Publ. Ind. Med. Assoc.* **1988**, *30*, 937.
[39] G. A. Hart, T. W. Hesterberg, *J. Occup. Environ. Med.* **1998**, *40*, 29.
[40] Shade of Aqua, Trend report *2020*, issue 1, https://exberry.com/newsletter/2020/EXBERRY_Trendreport_BlueCampagne_2020.pdf. (accessed: March 2021).

[41] M. He, J. P. Gales, É. Ducrot, Z. Gong, G.-R. Yi, S. Sacanna, D. J. Pine, *Nature* **2020**, *585*, 524.
[42] F. Garcıa-Santamarıa, C. Lopez, F. Meseguer, F. Lopez-Tejeira, J. Sanchez-Dehesa, H. Miyazaki, *Appl. Phys. Lett.* **2001**, *79*, 2309.
[43] P. V. Braun, R. Zehner, C. White, M. Weldon, C. Kloc, S. Patel, P. Wiltzius, *EPL* **2001**, *56*, 207.
[44] J. Zi, B. Dong, T. Zhan, X. Liu, *Bioinspiration*, Springer, Berlin **2012**, p. 275.
[45] R. O. Prum, R. Torres, S. Williamson, J. Dyck, *Proc. R. Soc. London, Ser. B.* **1999**, *266*, 13.
[46] R. O. Prum, R. H. Torres, S. Williamson, J. Dyck, *Nature* **1998**, *396*, 28.
[47] Y. Zhang, B. Dong, A. Chen, X. Liu, L. Shi, J. Zi, *Adv. Mater.* **2015**, *27*, 4719.
[48] J.-R. Gurr, A. S. Wang, C.-H. Chen, K.-Y. Jan, *Toxicology* **2005**, *213*, 66.
[49] X.-X. Chen, B. Cheng, Y.-X. Yang, A. Cao, J.-H. Liu, L.-J. Du, Y. Liu, Y. Zhao, H. Wang, *Small* **2013**, *9*, 1765.
[50] Z.-M. Song, N. Chen, J.-H. Liu, H. Tang, X. Deng, W.-S. Xi, K. Han, A. Cao, Y. Liu, H. Wang, *J. Appl. Toxicol.* **2015**, *35*, 1169.
[51] W.-S. Xi, Z.-M. Song, Z. Chen, N. Chen, G.-H. Yan, Y. Gao, A. Cao, Y. Liu, H. Wang, *Environ. Sci. Nano* **2019**, *6*, 565.
[52] A. Oomen, C. Rompelberg, M. Bruil, C. Dobbe, D. Pereboom, A. Sips, *Arch. Environ. Contam. Toxicol.* **2003**, *44*, 281.
[53] *Efsa J.* **2016**, *14*, 1512.